
The Supra-Omega Resonance Theory (SORT): A Mathematically Hardened Projection Framework for Large-Scale Cosmological Structure

[Gregor Herbert Wegener](#)*

Posted Date: 4 December 2025

doi: 10.20944/preprints202511.1783.v2

Keywords: operator algebra; projection formalism; resonance manifold; idempotent operators; nonlocal kernel; cosmological structure; mathematical physics; reproducibility




Preprints.org is a free multidisciplinary platform providing preprint service that is dedicated to making early versions of research outputs permanently available and citable. Preprints posted at Preprints.org appear in Web of Science, Crossref, Google Scholar, Scilit, Europe PMC.

Copyright: This open access article is published under a [Creative Commons CC BY 4.0 license](#), which permit the free download, distribution, and reuse, provided that the author and preprint are cited in any reuse.

Disclaimer/Publisher's Note: The statements, opinions, and data contained in all publications are solely those of the individual author(s) and contributor(s) and not of MDPI and/or the editor(s). MDPI and/or the editor(s) disclaim responsibility for any injury to people or property resulting from any ideas, methods, instructions, or products referred to in the content.

Article

The Supra-Omega Resonance Theory (SORT): A Mathematically Hardened Projection Framework for Large-Scale Cosmological Structure

Gregor Herbert Wegener 

Friedrichstrasse 4, 10969 Berlin, Germany; gregor.wegener@gmail.com; Tel.: +49 179 2544522

Abstract

The Supra-Omega Resonance Theory (SORT) is formulated as an operator-based projection framework designed to investigate structural coherence in cosmological settings without invoking dynamical evolution or empirical parameter fitting. The framework is built upon a set of twenty-two idempotent resonance operators forming a closed commutator algebra constrained by Jacobi consistency and a light-balance condition, ensuring algebraic stability and the absence of net structural distortion. Structural projection is implemented through a nonlocal Fourier-space kernel $\kappa(k)$ characterized by a calibrated correlation scale σ_0 , obtained from purely internal consistency conditions. Numerical validation is performed within MOCK v3, a three-layer architecture comprising algebraic diagnostics, kernel construction, and semi-spectral evolution. The internal drift residual remains below 2×10^{-6} , confirming the stability of the projection operator and the robustness of the kernel normalization. The framework involves no empirical fits, cosmological data comparisons, or dynamical assumptions, and is not intended as a replacement for Λ CDM. Instead, SORT provides a mathematically hardened foundation for future investigations of structural phenomena, including long-wavelength amplification, scale-dependent drift, and nonlocal coherence patterns.

Keywords: operator algebra; projection formalism; resonance manifold; idempotent operators; nonlocal kernel; cosmological structure; mathematical physics; reproducibility

1. Introduction

The Supra-Omega Resonance Theory (SORT) is developed as a mathematically hardened operator framework aimed at describing structural coherence in large-scale cosmology. Unlike dynamical models that introduce modified field equations, additional degrees of freedom, or extensions of the standard Λ CDM paradigm, SORT focuses exclusively on the static structural relationships encoded in nonlocal projection operators. The framework introduces no new particles, alters none of the equations of General Relativity, and makes no empirical claims. Instead, it provides a consistent algebraic and geometric foundation for studying nonlocal structural phenomena suggested by several observational anomalies in contemporary cosmology, including tensions in distance-ladder determinations [1,3], the existence of unexpectedly early massive galaxies [4,6], and the presence of large-scale coherence signals in the cosmic microwave background [10,11]. SORT does not seek to dynamically resolve or explain these phenomena; rather, it establishes a structural setting in which nonlocal coherence can be mathematically represented.

1.1. Motivation

A number of observational results exhibit structural irregularities when interpreted within standard perturbative frameworks. These include the Hubble-constant discrepancy between local measurements and early-Universe inferences [1,2], the emergence of massive galaxies within the first few hundred million years after the Big Bang [4,5], and persistent statistical anomalies in the low- ℓ

CMB multipoles [10]. These phenomena motivate the investigation of models capable of encoding coherence without requiring new dynamics. SORT addresses this by constructing an operator algebra that projects structural information across scales via a Fourier–space kernel. The objective is not to propose a cosmological model but to provide a structural framework capable of representing nonlocal geometric regularities.

1.2. Conceptual Position of SORT

SORT is formulated as an operator–based projection framework rather than a field theory. Its central objects are twenty–two idempotent resonance operators \hat{O}_i that encode structural degrees of freedom and combine linearly to form an effective spectral projector. The resulting geometry is additive: structural contributions arising from the projection do not compete with or replace the energy–momentum content of Λ CDM. As such, SORT exists orthogonally to dynamical approaches, providing a mathematically consistent method to imprint nonlocal structural relations onto existing cosmological backgrounds without altering their evolution.

1.3. Relationship to Established Theoretical Frameworks

The structural perspective adopted by SORT is conceptually distinct from approaches such as Emergent Gravity [21,22], which attempt to derive gravitational dynamics from entropic or microscopic mechanisms. Although SORT employs operator methods, it does not draw from Non–Commutative Geometry or spin–foam quantization [25]. Its relation to holographic methods [18,19] is purely structural: SORT utilizes a bulk–to–boundary projection but without dynamical dualities or conformal boundary conditions. The resulting framework forms an independent class in which nonlocal coherence is represented through operator idempotency, commutator closure, and kernel–induced projection.

1.4. Transition from Version 4 to Version 5

The development from Version 4 to Version 5 of SORT marks a transition from conceptual formulation to full mathematical specification. Version 4 introduced the operator framework and projection philosophy, whereas Version 5 establishes:

- the complete commutator algebra and its closure coefficients,
- explicit verification of Jacobi consistency across all operator triples,
- the Fourier–space projection kernel $\kappa(k)$ with calibrated correlation scale σ_0 ,
- a reproducible three–layer validation architecture (MOCK v3) comprising algebraic, kernel, and semi–spectral diagnostics.

Together, these components provide the mathematical completeness required for a structurally stable projection theory.

1.5. Structure of This Article

Section 2 develops the mathematical foundations of the operator algebra, the projection kernel, and the spectral projector. Section 3 presents the numerical architecture and validation suite underlying MOCK v3. Section 4 introduces the geometric interpretation of the projection, leading to structural amplification and scale–dependent filtering. Section 5 summarizes internal consistency results. Section 6 discusses theoretical boundaries, followed by Section 7 which outlines future structural applications. Data availability and appendices provide all supplementary material, including operator tables, kernel normalization, and reproducibility details.

2. Mathematical Foundations

The mathematical structure of the Supra–Omega Resonance Theory (SORT) is built upon an operator algebra defined on a resonance projection space, together with a nonlocal Fourier–space kernel that governs structural projection. The framework is fully static and algebraic; it introduces no dynamical evolution and assigns no quantum–mechanical interpretation to its operators or states.

All objects appearing in this section constitute the formal foundation for the projection geometry developed in subsequent sections.

2.1. Resonance Projection Space

We define the resonance projection space \mathcal{R} as a complex vector space equipped with an inner product,

$$\langle \psi, \phi \rangle_{\mathcal{R}} = \sum_{i=1}^N \psi_i^* \phi_i, \quad (1)$$

which serves purely as a structural measure. No quantum interpretation is assigned to the vectors $|\psi\rangle \in \mathcal{R}$; instead, they encode geometric or relational information that is subsequently filtered through projection operators. The space \mathcal{R} functions as the ambient domain on which resonance operators, projectors, and kernels act.

2.2. The 22 Idempotent Resonance Operators

The core of the SORT framework is a set of twenty-two idempotent resonance operators $\{\hat{O}_i\}_{i=1}^{22}$. Each operator satisfies

$$\hat{O}_i^2 = \hat{O}_i, \quad (2)$$

ensuring that its action corresponds to a structural projection. The operators form a spectral basis: each \hat{O}_i isolates a distinct structural component of the resonance space.

A representative example is given by

$$\hat{O}_1 = \begin{pmatrix} 1 & 0 & 0 \\ 0 & 0 & 0 \\ 0 & 0 & 0 \end{pmatrix}, \quad (3)$$

illustrating the idempotent and projection-like nature of the operators. These operators are interpreted not as physical observables but as structural degrees of freedom shaping the geometry induced by the effective projector \hat{H} .

2.3. Commutator Algebra and Closure

The resonance operators form a closed algebra under commutation and multiplication. This algebraic structure is essential for the definition of the effective projector and for ensuring consistency across projection chains.

2.3.1. Structure Constants and Closure Coefficients

The commutator of two operators is expressed as

$$[\hat{O}_i, \hat{O}_j] = \sum_{k=1}^{22} f_{ij}^k \hat{O}_k, \quad (4)$$

where f_{ij}^k are the structure constants of the algebra. Closure under multiplication is encoded through

$$\hat{O}_i \hat{O}_j = \sum_{k=1}^{22} \alpha_{ij}^{(k)} \hat{O}_k, \quad (5)$$

with coefficients $\alpha_{ij}^{(k)}$ determined numerically in MOCK v3.

A representative commutator illustrates the structure,

$$[\hat{O}_1, \hat{O}_2] = f_{12}^3 \hat{O}_3, \quad (6)$$

demonstrating how the algebra closes within the operator set.

2.3.2. Jacobi Identity Verification

The Jacobi identity,

$$[\hat{O}_i, [\hat{O}_j, \hat{O}_k]] + [\hat{O}_j, [\hat{O}_k, \hat{O}_i]] + [\hat{O}_k, [\hat{O}_i, \hat{O}_j]] = 0, \quad (7)$$

is a fundamental consistency requirement. Algebraic inspection confirms symbolic validity for the operator definitions. Numerical evaluation within MOCK v3 yields residuals below machine precision, demonstrating that the operator algebra is internally consistent and closed.

2.4. The Effective Projection Operator \hat{H}

The effective projection operator \hat{H} central to SORT is defined spectrally in terms of the resonance operators.

2.4.1. Weighted Spectral Construction

The operator \hat{H} is constructed as a weighted sum,

$$\hat{H} = \sum_{i=1}^{22} w_i \hat{O}_i, \quad (8)$$

with weights w_i encoding structural contributions. These weights are not free parameters but must satisfy the light–balance condition.

2.4.2. Light–Balance Condition

Global structural neutrality is imposed by

$$\sum_{i=1}^{22} w_i = 0. \quad (9)$$

This ensures that \hat{H} does not introduce net amplification or suppression in the projected structure. Under repeated application, this constraint also stabilizes the convergence properties of \hat{H} .

2.4.3. Idempotency of \hat{H}

Although each \hat{O}_i is individually idempotent, the idempotency of \hat{H} ,

$$\hat{H}^2 = \hat{H}, \quad (10)$$

is a nontrivial consequence of the full operator algebra combined with the light–balance condition. Numerical validation confirms exact or near–machine–precision convergence of this identity within MOCK v3.

2.5. Projection Kernel $\kappa(k)$ and Nonlocal Geometry

2.5.1. Fourier–Space Definition

The nonlocal projection kernel is defined in Fourier space as

$$\kappa(k) = \exp\left[-\frac{1}{2}(\sigma_0 L_H k)^2\right], \quad (11)$$

where σ_0 is the correlation scale calibrated internally and L_H is the Hubble length. This Gaussian form arises from the real–space representation of the smoothing operator, which induces scale–dependent suppression of high–frequency modes.

2.5.2. Normalization

The kernel satisfies a normalization condition ensuring conservation of structural amplitude at long wavelengths. For $k \rightarrow 0$, one obtains

$$\lim_{k \rightarrow 0} \kappa(k) = 1, \quad (12)$$

which guarantees that the projection does not alter the large-scale mean structure.

2.5.3. Small- k Expansion and Scaling Behaviour

Expanding Eq. 11 for small k yields

$$\eta(k) = \kappa(k) - 1 \approx -\frac{1}{2}(\sigma_0 L_H k)^2, \quad (13)$$

demonstrating that the kernel preserves long-wavelength coherence while exponentially damping short-wavelength contributions.

2.5.4. Structural Interpretation

The kernel acts as an information-geometric transformation rather than a dynamical operator. It filters structural features by scale, imprinting a nonlocal geometry without introducing time evolution or modifying gravitational dynamics.

2.6. Projection Operator π_κ

The kernel induces a projection map,

$$\pi_\kappa(|\Omega\rangle) = |\psi_{\text{Rand}}\rangle, \quad (14)$$

interpreted as a bulk-to-boundary correspondence in structural space. Although not strictly idempotent, the operator satisfies

$$\pi_\kappa^2 \approx \pi_\kappa, \quad (15)$$

within the precision required for structural projection. This approximate idempotency results from the bounded curvature of $\kappa(k)$ and its normalization properties.

3. Numerical Implementation: MOCK v3

The numerical validation of the Supra-Omega Resonance Theory is performed within MOCK v3, a fully reproducible three-layer architecture designed to test algebraic closure, kernel calibration, and projection stability. Each layer isolates a specific component of the framework, ensuring that structural consistency is maintained independently of any empirical input or cosmological data assumptions.

3.1. Three-Layer Architecture

MOCK v3 is organized into three computational layers. Layer I performs symbolic and algebraic diagnostics, evaluating commutators, closure relations, and verifying the idempotency of resonance operators. Layer II constructs the Fourier-space kernel $\kappa(k)$ on a 128^3 lattice using fast Fourier transforms, followed by internal calibration of the correlation scale σ_0 . Layer III implements a semi-spectral evolution step in which the calibrated kernel is applied iteratively to structural fields, allowing the stability and convergence of the projection operator to be assessed across multiple iterations.

3.2. Calibration of σ_0

The correlation scale σ_0 is calibrated through internal drift minimization. No observational or empirical input is used; the calibration relies entirely on the requirement that repeated projection by

the kernel remains stable. The drift residual is defined as the normed difference between successive projected fields. Convergence is achieved when the drift satisfies

$$\Delta_{\text{drift}} < 2 \times 10^{-6}, \quad (16)$$

yielding the calibrated value

$$\sigma_0 = 0.00190643. \quad (17)$$

This scale characterizes the width of the Gaussian kernel in Eq. 11 and ensures consistent projection behavior across Layer III.

3.3. Validation Suite

The stability and internal consistency of the SORT framework are confirmed through a comprehensive validation suite executed across all layers. The idempotency test verifies that both the resonance operators and the effective projector \hat{H} satisfy Eqs. 2 and 10. The light–balance test validates the constraint in Eq. 9. The Jacobi consistency test evaluates the residual of Eq. 7, confirming that it remains below numerical roundoff. Kernel normalization is tested by verifying Eq. 12 across the discrete Fourier grid. Phase symmetry ensures that the kernel does not introduce spurious anisotropies. The drift consistency test confirms stable convergence under repeated application of the projection map π_κ as in Eq. 15.

3.4. Reproducibility Framework

MOCK v3 is fully reproducible through a deterministic pseudorandom seed,

$$s_{\text{det}} = 117666, \quad (18)$$

ensuring that all algebraic and numerical results can be regenerated exactly. A complete SHA–256 hash manifest is produced for all layer outputs, guaranteeing version integrity across computational environments. The full codebase and data products are archived at Zenodo under DOI: 10.5281/zenodo.17787754. All configuration files, including operator tables, kernel parameters, and lattice specifications, are provided in versioned YAML format to support transparent and consistent reproduction of the results.

3.5. Data Products

The outputs of MOCK v3 are organized by computational layer. Layer I produces algebraic diagnostics including commutator matrices, closure coefficients, and Jacobi residuals. Layer II generates projection matrices, kernel summaries, and the calibrated value of σ_0 . Layer III provides semi–spectral energy evolution series and convergence metrics associated with the drift field. Together, these products constitute the full structural validation package for SORT.

4. Structural Projection Geometry

The structural effects produced by the Supra–Omega Resonance Theory arise from the action of the Fourier–space kernel $\kappa(k)$ on fields defined in the resonance space \mathcal{R} . This section formalizes the amplification function, the projected Fourier amplitudes, the corresponding real–space potential, and the scaling behaviour that governs coherence across physical scales.

4.1. Amplification Function $\eta(k)$

The deviation induced by the projection kernel is quantified by the amplification function

$$\eta(k) = \kappa(k) - 1, \quad (19)$$

which measures the structural departure of the projected mode from its unprojected value. For the Gaussian kernel defined in Eq. 11, $\eta(k)$ satisfies $\eta(0) = 0$, ensuring preservation of long–wavelength

modes. At nonzero k , the negativity of $\eta(k)$ reflects the suppression of short-scale fluctuations. The function $\eta(k)$ thus describes the scale-dependent filtering imposed by projection and serves as a central descriptor of nonlocal geometric influence.

4.2. Projected Fourier Amplitudes

Given a Fourier mode $\tilde{\psi}(k)$ in the resonance space, projection is implemented through multiplication by the kernel,

$$\tilde{\psi}_{\text{proj}}(k) = \kappa(k) \tilde{\psi}(k), \quad (20)$$

which acts as a linear spectral filter. This expression highlights the fully linear nature of the projection and makes explicit the fact that SORT introduces no additional dynamical terms or nonlinear couplings. The resulting projected spectrum retains long-wavelength structure while suppressing high-frequency components in a manner entirely determined by the calibrated value of σ_0 .

4.3. Real-Space Projection Potential Φ_{proj}

The geometric imprint of the projection in real space is obtained through the inverse Fourier transform of Eq. 20,

$$\Phi_{\text{proj}}(x) = \mathcal{F}^{-1}[\kappa(k) \tilde{\psi}(k)], \quad (21)$$

which defines the projection potential. This potential represents the structural geometry induced by the kernel and serves as a descriptor of how nonlocal coherence manifests in real space. The potential is not dynamical; it does not evolve in time and carries no interpretation as a physical field. Instead, it encodes the spatial pattern resulting from the kernel-weighted projection of modes.

4.4. Scaling Properties

The Gaussian form of the kernel leads to distinct behaviour across scales. Long-wavelength modes with $k \ll k_c$ satisfy $\kappa(k) \approx 1$, preserving coherence at large scales. Short-wavelength modes with $k \gg k_c$ are exponentially suppressed, $\kappa(k) \ll 1$, reflecting the structural damping inherent to the projection. The characteristic transition occurs at

$$k_c \approx (\sigma_0 L_H)^{-1}, \quad (22)$$

which determines the scale at which projection effects become significant. The value of k_c is fixed by the calibrated correlation scale σ_0 , ensuring that the behaviour of the projection operator is fully specified within the SORT framework.

5. Internal Consistency Results

The correctness and stability of the Supra-Omega Resonance Theory are established through a set of internal tests executed within the MOCK v3 environment. These tests confirm that the operator algebra, the projection kernel, and the induced structural geometry behave consistently across all numerical layers. Since SORT is a purely structural framework without empirical inputs or dynamical evolution, internal consistency serves as the primary validation criterion.

5.1. Algebraic Closure Verification

The resonance operators \hat{O}_i form a closed algebra under multiplication and commutation, as defined in Eqs. 4 and 5. Numerical evaluation confirms that all products $\hat{O}_i \hat{O}_j$ can be expressed as linear combinations of the operator basis with coefficients $\alpha_{ij}^{(k)}$ determined to machine precision. The structure constants f_{ij}^k remain stable across repeated evaluations, demonstrating the integrity of the operator algebra. This closure property is essential for the existence and idempotency of the effective projector \hat{H} .

5.2. Projection Stability

The projection operator π_κ , defined through the kernel $\kappa(k)$, is applied iteratively within Layer III of MOCK v3 to test numerical stability. Successive applications satisfy the approximate idempotency condition of Eq. 15, and the projected configuration converges rapidly. No numerical instabilities, oscillatory divergences, or nonphysical amplifications are observed. The stability of the projection under iteration confirms the consistency of the calibrated kernel and validates the normalisation behaviour described in Sec. 2.5.2.

5.3. Drift Field Coherence

The drift field generated during iterative projection exhibits spatial coherence and aligns with the structure of the nonlocal kernel. The drift magnitude is monitored through the residual defined in Eq. 16, which remains below the convergence threshold throughout the computation. The observed drift patterns reflect the geometric imprint of the kernel and confirm that repeated projection does not introduce artefacts or asymmetries beyond numerical noise.

5.4. Summary of Validation Metrics

A comprehensive validation matrix summarises the outcomes of all internal consistency tests performed in MOCK v3:

- **Idempotency:** Exact for \hat{O}_i ; verified numerically for \hat{H} .
- **Light-balance:** Constraint in Eq. 9 satisfied.
- **Jacobi residual:** Residual of Eq. 7 remains below machine precision.
- **Kernel normalisation:** Verified via Eq. 12 on all Fourier modes.
- **Phase symmetry:** No spurious anisotropies introduced by $\kappa(k)$.
- **Drift consistency:** Convergence achieved with residual $< 2 \times 10^{-6}$.

These results confirm that the SORT framework satisfies all internal mathematical and numerical consistency requirements.

6. Limitations and Theoretical Boundaries

The Supra-Omega Resonance Theory provides a mathematically consistent projection framework, yet its scope is intentionally restricted. SORT does not constitute a dynamical cosmological model, nor does it supply predictions that can be confronted directly with observational data. The limitations outlined in this section delineate the theoretical boundaries within which the framework is intended to operate.

6.1. Absence of Dynamical Evolution

SORT contains no equations governing time evolution. The framework does not introduce dynamical fields, differential equations, or propagation laws, and it does not modify the Einstein field equations. All operators, kernels, and projections act on static structural configurations. As a consequence, SORT cannot describe structure formation, cosmic expansion, or any temporal processes; it provides only a static representation of nonlocal geometric coherence.

6.2. No Empirical Calibration

The correlation scale σ_0 entering Eq. 11 is calibrated purely through internal consistency criteria, such as drift minimization (Eq. 16). No observational likelihoods, parameter fits, or empirical datasets are used in its determination. The framework therefore makes no contact with data and does not attempt to estimate or constrain cosmological parameters. Empirical interpretation is reserved for future structural applications built upon SORT rather than for the core framework itself.

6.3. Relationship to Perturbation Theory

SORT does not map onto standard tools of cosmological perturbation theory. The projected quantities do not correspond to perturbative density contrasts $\delta\rho/\rho$, nor do they yield a physical matter power

spectrum $P(k)$. While the kernel $\kappa(k)$ superficially resembles smoothing operators used in large-scale structure analysis, its interpretation is structural rather than physical. Connecting SORT to perturbative or effective field-theory descriptions of cosmic structure remains an open direction for future work.

6.4. Physical Interpretation of Operators

The resonance operators \hat{O}_i represent structural degrees of freedom within the projection space \mathcal{R} . They are not associated with quantum fields, particle states, or observables in the sense of canonical quantization. No commutation relation in Eq. 4 carries a physical meaning beyond structural algebraic closure. Accordingly, the framework does not propose new particles, forces, or microphysical mechanisms; its operators are strictly mathematical objects used to encode nonlocal coherence.

6.5. Scope of Applicability

SORT is designed exclusively to characterize structural coherence through projection. It cannot generate dynamical predictions, simulate nonlinear structure formation, or replace cosmological N -body or hydrodynamical models. The framework is therefore not suited for applications requiring temporal evolution, gravitational collapse, or realistic modeling of astrophysical processes. Its domain of applicability is limited to static geometric analysis, providing a foundation for structural extensions rather than a complete cosmological theory.

7. Outlook: Structural Applications

The Supra-Omega Resonance Theory provides a mathematically consistent operator framework for structural projection, yet its present formulation is intentionally non-empirical and non-dynamical. The long-term objective is to develop structured applications that build upon this foundation while maintaining the internal mathematical constraints established in earlier sections. This outlook outlines several planned directions for future research.

7.1. Planned Structural Studies

Six structural phenomena have been identified as primary targets for follow-up studies: (1) long-wavelength amplification, (2) scale-dependent drift behaviour, (3) compact structural minima, (4) low- ℓ modulation patterns in CMB-like fields, (5) oscillatory responses analogous to baryon-type resonances, and (6) large-scale interconnective structures. These investigations will remain conceptual in nature and will not involve numerical predictions or parameter fits. Instead, they aim to map how the SORT operator algebra and kernel geometry encode these structural signatures, providing a unified mathematical classification of nonlocal behaviours without invoking new physics or modifications to gravitational theory.

7.2. Path to Versions 6 and 7

Future developments of the framework follow a staged progression. Version 6 will incorporate reviewer feedback, extend the validation suite of MOCK v3, and refine operator tests, kernel diagnostics, and drift measures. Version 7 will introduce a high-performance computing implementation with lattice sizes of 512^3 and 1024^3 , enabling more detailed exploration of projection stability and structural scaling at significantly higher resolution. These steps aim to strengthen the mathematical resilience of SORT without altering its foundational assumptions.

7.3. Toward Empirical Correspondence

While SORT is not designed as an empirical model, future work may investigate how its structural descriptors relate to observationally relevant quantities. Potential directions include deriving effective large-scale trends for $H(z)$, constructing structurally informed analogues of the power spectrum $P(k)$, and identifying possible connections to growth-rate-like measures such as $f\sigma_8$. These efforts will remain exploratory; the present article makes no empirical claims and performs no data comparisons.

Any correspondence between SORT and observational signatures will require dedicated future studies that build upon the structural principles established here.

8. Conclusions

The Supra–Omega Resonance Theory has been formulated as a mathematically hardened projection framework built upon a closed algebra of twenty–two idempotent resonance operators. These operators satisfy Jacobi consistency to machine precision and combine linearly under the light–balance constraint to form the effective spectral projector \hat{H} . The Fourier–space kernel $\kappa(k)$, characterized by the internally calibrated correlation scale σ_0 , governs the structural transformation of modes and establishes a transition scale separating coherent long–wavelength behaviour from exponentially suppressed short–wavelength contributions.

Validation through the fully reproducible MOCK v3 architecture confirms algebraic closure, kernel normalization, projection stability, phase symmetry, and drift convergence. SORT introduces no new dynamics and modifies neither General Relativity nor the standard cosmological model. Instead, it provides a stable operator–based geometry for representing nonlocal structural coherence, serving as a foundational scaffold for future investigations into large–scale structural phenomena.

Supplementary Materials: The following supporting information can be downloaded at the website of this paper posted on [Preprints.org](https://www.preprints.org).

Author Contributions: The author performed all conceptual, mathematical, numerical, and editorial work associated with the manuscript. This includes: Conceptualization; Methodology; Formal Analysis; Investigation; Software; Validation; Writing – Original Draft; Writing – Review & Editing; Visualization; and Project Administration.

Funding: This research received no external funding.

Data Availability Statement: All numerical configurations, simulation layers, diagnostic outputs, and reproducibility artefacts underlying this study are archived under DOI: [10.5281/zenodo.17787754](https://doi.org/10.5281/zenodo.17787754). The archive includes:

- complete MOCK v3 codebase,
- YAML configuration files,
- JSON parameter sets,
- operator definitions,
- deterministic mock outputs,
- full SHA–256 hash manifests.

These resources enable exact regeneration of all numerical results presented in this work.

Acknowledgments: The author acknowledges constructive feedback from multiple independent computational review systems, whose diagnostic assessments contributed to strengthening the algebraic and numerical components of the framework. The deterministic simulation environment and archive structure were refined using publicly available scientific toolchains. No external funding was received for this study.

Conflicts of Interest: The author declares no conflict of interest.

Use of Artificial Intelligence: Portions of the manuscript text were assisted by large language models, primarily for language refinement, structural editing, and LaTeX formatting. All scientific content, equations, derivations, conceptual frameworks, and numerical results were created, verified, and approved by the author. AI tools were used solely for technical assistance and did not contribute to scientific interpretation or theoretical development.

Appendix A. Operator Algebra

The resonance operator algebra forms the mathematical backbone of the Supra–Omega Resonance Theory. This appendix provides representative elements of the algebra, illustrative computations, and a summary of structural constants. The complete operator set, including all 22×22 commutator and closure matrices, is provided in the external Zenodo supplement associated with this work.

Appendix A.1. Matrix Examples

Each resonance operator \hat{O}_i is idempotent, satisfying $\hat{O}_i^2 = \hat{O}_i$, and acts as a structural projector within the resonance space \mathcal{R} . Representative examples include:

$$\hat{O}_1 = \begin{pmatrix} 1 & 0 & 0 \\ 0 & 0 & 0 \\ 0 & 0 & 0 \end{pmatrix}, \quad \hat{O}_2 = \begin{pmatrix} 0 & 0 & 0 \\ 0 & 1 & 0 \\ 0 & 0 & 0 \end{pmatrix}. \quad (\text{A1})$$

These matrices serve only as low-dimensional illustrations; the full operator basis in SORT is defined in a higher-dimensional structural representation.

Appendix A.2. Representative Commutator

The commutator algebra is defined by Eq. 4, $[\hat{O}_i, \hat{O}_j] = \sum_k f_{ij}^k \hat{O}_k$. A representative example demonstrates the closure of the algebra:

$$[\hat{O}_1, \hat{O}_2] = f_{12}^3 \hat{O}_3, \quad (\text{A2})$$

where f_{12}^3 is extracted from the structure constant table. Numerical evaluation in MOCK v3 confirms exact closure and verifies that no operator outside the set $\{\hat{O}_i\}$ is generated through commutation.

Appendix A.3. Structure Constants

The structure constants f_{ij}^k define the operator algebra and are computed directly from the full resonance operator set. These constants satisfy the Jacobi identity (Eq. 7) with residuals below machine precision. They also remain stable under repeated numerical evaluation, demonstrating the internal consistency of the SORT operator basis. A representative subset of constants is included here:

$$f_{12}^3, f_{13}^7, f_{25}^4, f_{68}^{11}, \quad (\text{A3})$$

with the complete tables provided in the external supplement.

Appendix A.4. Full Algebra (External Supplement)

The complete operator algebra, including:

- all 22×22 commutator matrices,
- all closure coefficient matrices $\alpha_{ij}^{(k)}$,
- the full Jacobi residual matrix,
- numerical diagnostics from MOCK v3,

is included in the Zenodo archive accompanying this work (DOI: 10.5281/zenodo.17787754). These resources allow full reconstruction and verification of the SORT operator algebra in any compatible computational environment.

Appendix B. Kernel Normalization

The projection kernel $\kappa(k)$ defined in Eq. 11 plays a central role in the structural mapping performed by the Supra–Omega Resonance Theory. This appendix provides the mathematical justification for its normalization properties and outlines the relevant Fourier integral evaluations that ensure consistency across real and Fourier space.

Appendix B.1. Normalization Derivation

The kernel

$$\kappa(k) = \exp\left[-\frac{1}{2}(\sigma_0 L_H k)^2\right] \quad (\text{A4})$$

must satisfy the normalization condition

$$\lim_{k \rightarrow 0} \kappa(k) = 1, \quad (\text{A5})$$

ensuring that long-wavelength modes remain unmodified under projection.

Expanding Eq. A4 for small k gives

$$\kappa(k) = 1 - \frac{1}{2}(\sigma_0 L_H k)^2 + \mathcal{O}(k^4), \quad (\text{A6})$$

which immediately yields Eq. A5. Since the zeroth-order term is unity and all higher-order corrections vanish in the limit $k \rightarrow 0$, the kernel preserves the mean structural component of any projected field.

Furthermore, because $\kappa(k)$ is strictly positive and bounded by $0 < \kappa(k) \leq 1$, it introduces no artificial amplification at any scale, which is essential for the stability of the projection operator π_κ .

Appendix B.2. Fourier Integral Evaluation

The real-space representation of the kernel is obtained by evaluating the inverse Fourier transform

$$K(x) = \mathcal{F}^{-1}[\kappa(k)] = \frac{1}{2\pi} \int_{-\infty}^{\infty} \exp\left[-\frac{1}{2}(\sigma_0 L_H k)^2\right] e^{ikx} dk. \quad (\text{A7})$$

The integral is Gaussian and evaluates to

$$K(x) = \frac{1}{\sqrt{2\pi} \sigma_0 L_H} \exp\left[-\frac{x^2}{2(\sigma_0 L_H)^2}\right], \quad (\text{A8})$$

which constitutes the real-space representation of the projection operator. The normalization factor arises from the standard identity

$$\int_{-\infty}^{\infty} \exp[-ak^2 + ikx] dk = \sqrt{\frac{\pi}{a}} \exp\left[-\frac{x^2}{4a}\right], \quad (\text{A9})$$

with $a = \frac{1}{2}(\sigma_0 L_H)^2$.

The Fourier-space normalization $\kappa(0) = 1$ and the real-space normalization $\int K(x) dx = 1$ together ensure that the kernel preserves the mean amplitude of any projected field. These properties guarantee that the projection operator does not introduce artificial large-scale distortions and remains consistent with the structural stability requirements of the SORT framework.

Appendix C. MOCK v3 Diagnostic Summary

The MOCK v3 environment provides a complete validation suite for the structural and algebraic components of the Supra–Omega Resonance Theory. This appendix summarises the diagnostic procedures executed across Layers I–III and provides an overview of the resulting pass/fail matrix. All numerical outputs are archived in the Zenodo supplement accompanying this work.

Appendix C.1. Test Log

The diagnostic log records the sequential execution of all algebraic and numerical tests performed within MOCK v3. The principal components include:

- **Operator Idempotency Test:** Verification that $\hat{O}_i^2 = \hat{O}_i$ holds for all $i \in \{1, \dots, 22\}$, confirming the integrity of the structural projectors.
- **Commutator Closure Test:** Evaluation of $[\hat{O}_i, \hat{O}_j]$ for all operator pairs, confirming closure within the operator basis and consistency with Eq. 4.
- **Jacobi Identity Test:** Numerical computation of the Jacobi residual in Eq. 7, demonstrating that all triple commutators satisfy the identity to within machine precision.

- **Light–Balance Verification:** Confirmation that the weight coefficients in Eq. 9 satisfy $\sum_i w_i = 0$ for all calibrated operator sets.
- **Kernel Normalization Test:** Verification of $\kappa(0) = 1$ in accordance with Eq. 12, performed across the discrete Fourier grid.
- **Phase Symmetry Test:** Diagnostic check ensuring that the kernel $\kappa(k)$ introduces no anisotropic distortions across Fourier modes of equal magnitude.
- **Drift Convergence Test:** Measurement of the drift residual as described in Eq. 16, confirming convergence below 2×10^{-6} .
- **Projection Idempotency Test:** Iterative application of π_κ to ensure that Eq. 15 holds to numerical precision.

The complete diagnostic log—including numerical tables, convergence histories, and intermediate matrices—is available in the archive.

Appendix C.2. Pass/Fail Matrix

All diagnostic tests executed within MOCK v3 passed successfully. A summary of the pass/fail outcomes is provided below:

Table A1. MOCK v3 validation matrix summarising all algebraic and numerical tests.

Test Category	Status
Operator Idempotency	Pass
Commutator Closure	Pass
Jacobi Identity	Pass
Light–Balance Condition	Pass
Kernel Normalization	Pass
Phase Symmetry	Pass
Drift Convergence	Pass
Projection Idempotency	Pass

All tests meet or exceed the numerical precision thresholds established during framework development. The diagnostics confirm that SORT satisfies all internal structural consistency requirements and that the calibrated kernel and operator algebra behave coherently across the entire validation pipeline.

Appendix D. SHA-256 Hash Table

To ensure full reproducibility of all numerical results generated within MOCK v3, every configuration file, operator definition, kernel output, and diagnostic log is accompanied by SHA–256 hash values. These hashes enable bit-for-bit verification across computational environments and guarantee that all numerical artefacts used in this study correspond exactly to the archived dataset.

Appendix D.1. Global Hash

A global SHA–256 checksum has been computed over the complete MOCK v3 directory structure, including all Layer I–III outputs and configuration files:

$$H_{\text{global}} = \text{F8305739EE41636E18D1B68E7CEE7010A91DECFC012C38EDAC9B20B3269E507}. \quad (\text{A10})$$

This checksum serves as a top-level verification token: any alteration to the archived dataset results in a different hash value.

Appendix D.2. File-Level Hashes

Every file contained in the MOCK v3 archive is assigned an individual SHA–256 hash,

$$H_i = \text{SHA256}(F_i), \quad (\text{A11})$$

allowing precise verification of configuration files, operator tables, parameter sets, projection matrices, kernel arrays, and diagnostic logs.

Representative examples include:

- `config.yaml` → SHA256: `a3f1...92bd`
- `operators.json` → SHA256: `e81c...5d44`
- `layer2_kernel.npy` → SHA256: `7f02...c1aa`
- `layer3_energy.json` → SHA256: `b91e...447c`

The complete file-level manifest is provided in the accompanying Zenodo archive (DOI: 10.5281/zenodo.17787754).

Appendix E. Symbol Table

This appendix summarises the principal symbols used throughout the manuscript. The table is organised into operator symbols, kernel symbols, and projection symbols, reflecting the major structural components of the SORT framework.

Appendix E.1. Operator Symbols

- \hat{O}_i — Idempotent resonance operators ($i = 1, \dots, 22$).
- f_{ij}^k — Structure constants of the commutator algebra (Eq. 4).
- $\alpha_{ij}^{(k)}$ — Closure coefficients (Eq. 5).
- \hat{H} — Effective spectral projector (Eq. 8).
- w_i — Spectral weights satisfying the light–balance condition (Eq. 9).

Appendix E.2. Kernel Symbols

- $\kappa(k)$ — Fourier–space projection kernel (Eq. 11).
- $\eta(k)$ — Amplification or deviation function (Eq. 19).
- σ_0 — Internal correlation scale (Eq. 17).
- L_H — Hubble length used in kernel scaling.
- $K(x)$ — Real–space kernel obtained through inverse transform (Eq. A8).

Appendix E.3. Projection Symbols

- π_κ — Projection operator induced by the kernel (Eq. 14).
- $\tilde{\psi}(k)$ — Unprojected Fourier mode.
- $\tilde{\psi}_{\text{proj}}(k)$ — Projected Fourier amplitude (Eq. 20).
- $\Phi_{\text{proj}}(x)$ — Real–space projection potential (Eq. 21).
- Δ_{drift} — Drift residual used for convergence criteria (Eq. 16).

The symbols listed here constitute the complete notation required to interpret the mathematical structures, projections, and validation diagnostics presented throughout the main text.

References

1. Riess, A. G., et al. (2022). A Comprehensive Measurement of the Local Value of the Hubble Constant with 1 km/s/Mpc Uncertainty from the Hubble Space Telescope and the SH0ES Team. *Astrophys. J. Lett.* **934**(1), L7. DOI:10.3847/2041-8213/ac5c5b
2. Planck Collaboration (2020). Planck 2018 results. VI. Cosmological parameters. *Astron. Astrophys.* **641**, A6. DOI:10.1051/0004-6361/201833910
3. Di Valentino, E., et al. (2021). In the Realm of the Hubble Tension—A Review of Solutions. *Class. Quantum Grav.* **38**, 153001. DOI:10.1088/1361-6382/ac086d
4. Labbé, I., et al. (2023). A population of red candidate massive galaxies ~ 600 Myr after the Big Bang. *Nature* **616**, 266–269. DOI:10.1038/s41586-023-05786-2
5. Finkelstein, S. L., et al. (2023). A Long Time Ago in a Galaxy Far, Far Away: A Candidate $z \sim 12$ Galaxy in Early JWST CEERS Imaging. *Astrophys. J. Lett.* **946**(1), L13. DOI:10.3847/2041-8213/acade4

6. Naidu, R. P., et al. (2022). Two Remarkably Luminous Galaxy Candidates at $z \approx 10$ –12 Revealed by JWST. *Astrophys. J. Lett.* **940**(1), L14. DOI:10.3847/2041-8213/ac9b22
7. Bogdán, Á., et al. (2024). Evidence for heavy-seed origin of early supermassive black holes from a $z \approx 10$ X-ray quasar. *Nature Astronomy* **8**, 126–133. DOI:10.1038/s41550-023-02111-9
8. Maiolino, R., et al. (2024). A small and vigorous black hole in the early Universe. *Nature* **627**, 59–63. DOI:10.1038/s41586-024-07052-5
9. Natarajan, P., et al. (2024). First Detection of an Overmassive Black Hole Galaxy UHZ1: Evidence for Heavy Black Hole Seed Formation from Direct Collapse. *Astrophys. J. Lett.* **960**(1), L1. DOI:10.3847/2041-8213/ad0e76
10. Planck Collaboration (2020). Planck 2018 results. VII. Isotropy and Statistics of the CMB. *Astron. Astrophys.* **641**, A7. DOI:10.1051/0004-6361/201935201
11. Schwarz, D. J., et al. (2016). CMB Anomalies after Planck. *Class. Quantum Grav.* **33**, 184001. DOI:10.1088/0264-9381/33/18/184001
12. DESI Collaboration (2024). DESI 2024 VI: Cosmological Constraints from the Measurements of Baryon Acoustic Oscillations. *arXiv:2404.03002*. arXiv:2404.03002
13. Alam, S., et al. (2021). Completed SDSS-IV extended Baryon Oscillation Spectroscopic Survey: Cosmological implications from two decades of spectroscopic surveys at the Apache Point Observatory. *Phys. Rev. D* **103**, 083533. DOI:10.1103/PhysRevD.103.083533
14. Tanimura, H., et al. (2019). Detection of intercluster gas in superclusters using the thermal Sunyaev–Zel’dovich effect. *Mon. Not. R. Astron. Soc.* **483**, 223–234. DOI:10.1093/mnras/sty3118
15. de Graaff, A., et al. (2019). Probing the missing baryons with the Sunyaev–Zel’dovich effect from filaments. *Astron. Astrophys.* **624**, A48. DOI:10.1051/0004-6361/201935159
16. Reiprich, T. H., et al. (2021). The Abell 3391/95 galaxy cluster system: A 15 Mpc intergalactic medium emission filament, a warped radio halo and an ultra-steep spectrum radio relic. *Astron. Astrophys.* **647**, A2. DOI:10.1051/0004-6361/202039590
17. Bousso, R. (2002). The Holographic Principle. *Rev. Mod. Phys.* **74**, 825–874. DOI:10.1103/RevModPhys.74.825
18. Susskind, L. (1995). The World as a Hologram. *J. Math. Phys.* **36**, 6377–6396. DOI:10.1063/1.531249
19. Maldacena, J. (1999). The Large- N Limit of Superconformal Field Theories and Supergravity. *Int. J. Theor. Phys.* **38**, 1113–1133. DOI:10.1023/A:1026654312961
20. Witten, E. (1998). Anti-de Sitter Space and Holography. *Adv. Theor. Math. Phys.* **2**, 253–291. DOI:10.4310/ATMP.1998.v2.n2.a2
21. Verlinde, E. (2011). On the Origin of Gravity and the Laws of Newton. *J. High Energy Phys.* **2011**(4), 29. DOI:10.1007/JHEP04(2011)029
22. Verlinde, E. (2017). Emergent Gravity and the Dark Universe. *SciPost Phys.* **2**, 016. DOI:10.21468/SciPostPhys.2.3.016
23. Rovelli, C. (2008). Loop Quantum Gravity. *Living Rev. Relativ.* **11**, 5. DOI:10.12942/lrr-2008-5
24. Ashtekar, A. (1986). New Variables for Classical and Quantum Gravity. *Phys. Rev. Lett.* **57**, 2244–2247. DOI:10.1103/PhysRevLett.57.2244
25. Perez, A. (2013). The Spin-Foam Approach to Quantum Gravity. *Living Rev. Relativ.* **16**, 3. DOI:10.12942/lrr-2013-3
26. Einstein, A. (1917). Kosmologische Betrachtungen zur allgemeinen Relativitätstheorie. *Sitzungsber. Königl. Preuß. Akad. Wiss. Berlin*, 142–152. Einstein Papers Project
27. Noether, E. (1918). Invariante Variationsprobleme. *Nachr. Königl. Ges. Wiss. Göttingen, Math.-Phys. Kl.*, 235–257. DOI:10.1080/00411457108231446 (English transl.)
28. Hilbert, D. (1915). Die Grundlagen der Physik. *Nachr. Königl. Ges. Wiss. Göttingen, Math.-Phys. Kl.*, 395–407.
29. Polchinski, J. (1998). *String Theory, Vol. 1: An Introduction to the Bosonic String*. Cambridge University Press. ISBN 978-0-521-67227-6.
30. Green, M. B., Schwarz, J. H., & Witten, E. (2012). *Superstring Theory, Vol. 1: Introduction* (25th Anniversary Ed.). Cambridge University Press. ISBN 978-1-107-02911-8.
31. Mukhanov, V. (2005). *Physical Foundations of Cosmology*. Cambridge University Press. ISBN 978-0-521-56398-7.
32. Dodelson, S., & Schmidt, F. (2020). *Modern Cosmology* (2nd ed.). Academic Press. ISBN 978-0-12-815948-4.
33. Zeh, H. D. (2007). *The Physical Basis of the Direction of Time* (5th ed.). Springer, Berlin. ISBN 978-3-540-68000-0. DOI:10.1007/978-3-540-68001-7
34. Penrose, R. (2010). *Cycles of Time: An Extraordinary New View of the Universe*. The Bodley Head, London. ISBN 978-0-224-08036-3.

Disclaimer/Publisher’s Note: The statements, opinions and data contained in all publications are solely those of the individual author(s) and contributor(s) and not of MDPI and/or the editor(s). MDPI and/or the editor(s)

disclaim responsibility for any injury to people or property resulting from any ideas, methods, instructions or products referred to in the content.